DYNAMIC IMPACT OF A CERAMIC SKELETON OF INTERPENETRATING PHASE COMPOSITES

Eligiusz Postek *[1], Tomasz Sadowski[2], Jarosław Bieniaś [2], Marek Boniecki[3]
[1] Institute of Fundamental Technological Research, Polish Academy of Science, Warsaw, Poland
[2] Department of Civil Engineering and Architecture, Lublin University of Technology, Lublin, Poland
[3] Institute of Electronic Materials Technology, Warsaw, Poland

Summary The paper presents modelling of a ceramic foam that works as skeleton of Interpenetrating Phase Composites (IPCs) before filling the preforms. The preforms are made of SiC or Al_2O_3. A dynamic analysis of an impact of such skeletons against rigid surface is performed. The results of the quasi-static analysis will serve as a reference to the dynamic analyses. The analysis of the IPCs skeleton is performed due to evaluation of the role of the skeleton in final product that is the filled IPCs.

INTRODUCTION AND MOTIVATION

Contemporary ceramic composites are used in many industries of strategic importance, such as the armaments industry, aviation, automotive [1] nuclear power [2] or space exploration, while in other areas they constitute the main source of technical progress [3]. In these applications, the material is often subjected to extreme loads, such as variable shock loads and high temperatures. In the presentation, we explore the degradation of an IPC skeleton.

In the last twenty years, the peridynamics that is a meshless non-local has been developed [4]. The method appears to be useful in analysis of brittle materials. The Metal-Ceramic composites are analysed in [5]. Metallic foams are analysed in [6].

NUMERICAL MODELLING

Problem statement

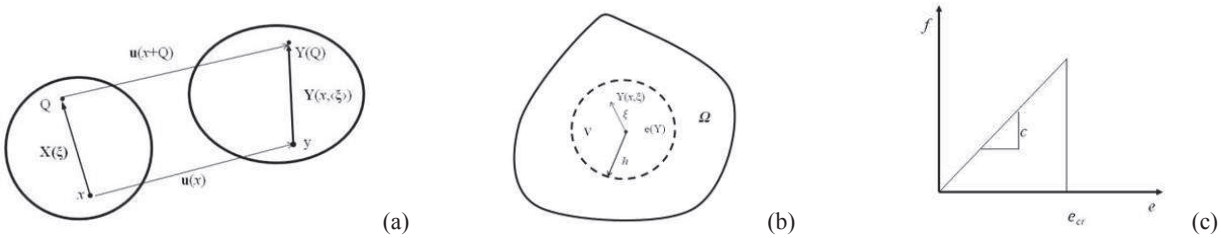

Figure 1. Peridynamics: state of deformation (a), integration over horizon (b), dependence of a force on stretch in a single bond (c).

When observing Fig. 1(a), x and Q are points in the undeformed body. It is a bond definition, $\xi = Q - x$. A reference state $\mathbf{X}$ is a function that acts on a bond, $\mathbf{X}(\xi)$. The deformation state depends on the new position of the coordinate x in the deformed configuration $y(x)$) as follows,$\mathbf{Y}(x, \xi) = y(x + \xi) - y(x)$. It yields $\mathbf{Y}(x, \xi) = y(Q) - y(x)$. The displacement state $U(x, \xi) = \boldsymbol{u}(x + \xi) - \boldsymbol{u}(\xi)$ yields $U(x, \xi) = \boldsymbol{u}(Q) - \boldsymbol{u}(x)$. Following Fig. 1(a), the scalar extension state $e(\boldsymbol{Y})$ is given as follows:

$$e(\mathbf{Y}) = |\mathbf{Y}| - |\mathbf{X}|$$

The scalar extension state is decomposed into its spherical e^i and deviatoric e^d parts:

$$e = e^i + e^d$$

The elastic force state $t(Y)$ is given in the form analogous to standard stress strain relation being the sum of the spherical and deviatoric parts as follows:

$$t(Y) = (3k\theta/m)\omega\underline{x} + \alpha\omega e^d$$

where k is the bulk modulus, θ is the dilatation, m is the weighted volume, ω is the influence function, $x = |\xi|$ is the basic scalar state, α is the coefficient related to the shear modulus $\alpha = (15\mu)/m$ where μ is the shear modulus.

The assumptions for the material failure model are as follows [7]. Bonds fail when their extension exceeds a critical value. Damage is caused by accumulation of broken bonds. Bonds failure is irreversible. A scheme for a single bond is shown in Fig 1(c) . The integration is over a domain V for all bonds. The dependence of force on its stretch in a bond is given in Fig. 1(b). It reads:

$$f = ce\zeta$$

where c is a constant depending on bulk modulus k and radius of the horizon h, $c = (18k)/(\pi h^4)$. Function is history dependent (time t) and takes value 1 when bond stretch is lower than critical stretch ζ or 0 otherwise. The damage d is defined s follows:

$$d(x,t) = 1 - \int_V \zeta(x,t,\xi)dV \Big/ \int_V dV$$

where *d* varies between 0 for primordial material and 1 for fully damaged material.

Physical model

The AL_2O_3 preforms are shown in Fig. 2(a) and Fig 2(b). The performs are of large pores and small pores, respectively. To obtain a numerical model, the CT scans of the performs are performed. The scans are shown Fig. 2(c) and Fig. 2(b). Basing on the CT scans, the hexadral discretizations are obtained. The initial discretizations stands for a base of finite element an peridynamics numerical models.

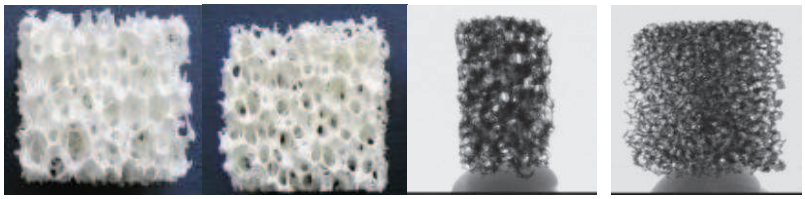

(a) (b) (c) (d)

Figure 2. Physical model: large pores sample (a), small pores sample (b), CT scan of large pores sample (c), CT scan of small pores sample.

Numerical model

The peridynamics models of the large and small pores samples are shown in Fig. 3. The impact scheme against the rigid surface is shown in Fig. 3(a). In this case, the impact velocity is 100 m/s. The damage development is shown in Fig. 3(b) and Fig 3(c) at time 9.5E-07 s. The difference in the range is clearly visible, the small pores sample is significantly more damaged than the large pores sample. The small pore sample is practically damaged in contrast to the large pores sample.

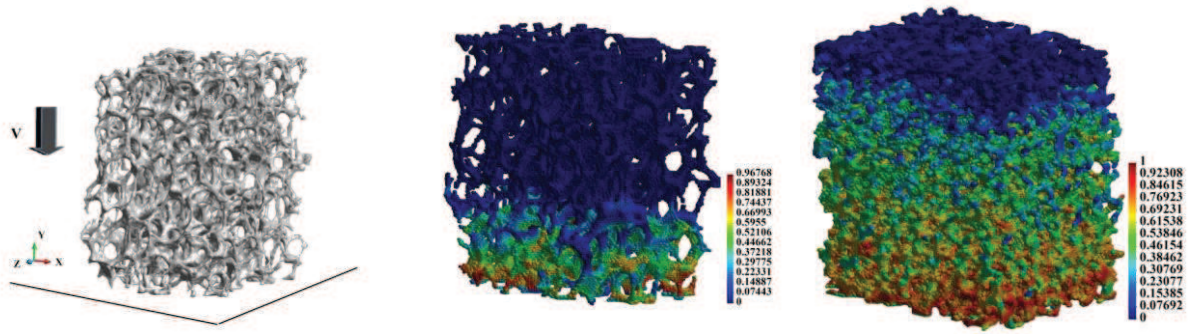

(a) (b) (c)

Figure 3. Damage distribution, impact velocity 100 m/s: a) impact scheme, b) large pores case, c) small pores case.

CONCLUSION AND FINAL REMARKS

We presented an application of peridynamics method for damage evaluation of the IPC skeleton. The damage development depends on porosity of the preforms strongly. It will be reflected in the final product as well. The calculations of the systems practically cannot be performed without application of High Performance Computing (HPC).

Acknowledgment

The results presented in this paper were obtained within the framework of research grant 2018/31/B/ST8/00601 financed by the National Science Centre, Poland. Calculations are performed using the "Okeanos" Cray CX40 system at the Interdisciplinary Centre for Mathematical and Computational Modelling in the University of Warsaw, Poland.

References

[1] Okada A. *Materials Science and Engineering B*, **161**: 182, 2009.
[2] Pittari J., Subhash G., Zheng J., Halls V., Jannotti P. *Journal of the European Ceramic Society*, **35**: 4411, 2015.
[3] Saberi Y., Zebarjad S.M., Akbari G.H. *Journal of Alloys and Compounds*, **484**: 637, 2009.
[4] Silling S. A. *Journal of the Mechanics and Physics of Solids*, **175**: 48, 2000.
[5] Sadowski T., Pankowski B. *Composite Structures,* **143:** 388, 2016.
[6] Postek E., Pęcherski R., Nowak Z. *Archives of Metallurgy and Materials*, **64**: 1603, 2019.
[7] Silling S.A., Epton M., Weckener O., Xu J., Askari E., *Journal of Elasticity,* **88**: 151, 2007.